Weierstraß-Institut
für Angewandte Analysis und Stochastik

im Forschungsverbund Berlin e.V.

Preprint ISSN 0946 – 8633

Kinetic Schemes for Selected Initial and Boundary Value Problems

Wolfgang Dreyer[1], Michael Herrmann[1],

Matthias Kunik[2], Shamsul Qamar[1]

submitted: 17 Oct 2003

[1] Weierstrass Institute
for Applied Analysis
and Stochastics
Mohrenstraße 39
10117 Berlin
Germany
dreyer@wias-berlin.de
herrmann@wias-berlin.de
qamar@wias-berlin.de

[2] Institute for Analysis and Numerics
Faculty of Mathematics
Otto-von-Guericke University Magdeburg
Postfach 4120
39016 Magdeburg
Germany
matthias.kunik@mathematik.uni-magdeburg.de

No. 880

Berlin 2003

2000 *Mathematics Subject Classification.* 76Y05, 82C40, 82C70.

Key words and phrases. Maximum Entropy Principle, Extended Thermodynamics, kinetic schemes, relativistic Euler equations, conservation laws, hyperbolic systems, shock waves, kinetic theory of phonons .

This project is granted by the DFG Priority Research Program "Analysis and Numerics for Conservation Laws".

Edited by
Weierstraß-Institut für Angewandte Analysis und Stochastik (WIAS)
Mohrenstraße 39
10117 Berlin
Germany

Fax: + 49 30 2044975
E-Mail: preprint@wias-berlin.de
World Wide Web: http://www.wias-berlin.de/

Abstract

The hyperbolic system that describes heat conduction at low temperatures and the relativistic Euler equations belong to a class of hyperbolic conservation laws that result from an underlying kinetic equation. The focus of this study is the establishment of an kinetic approach in order to solve initial and boundary value problems for the two examples. The ingredients of the kinetic approach are: (i) Representation of macroscopic fields by moment integrals of the kinetic phase density. (ii) Decomposition of the evolution into periods of free flight, which are interrupted by update times. (iii) At the update times the data are refreshed by the Maximum Entropy Principle.

1 Introduction

In this article we study (i) initial value problems for kinetic equations and (ii) initial and boundary value problems for the corresponding hyperbolic moment systems. We consider two different physical phenomena that, however, lead to similar equations which can be solved by kinetic schemes.

1. The evolution of heat in crystalline solids at low temperature is driven by the transport of phonons, which form a gas like structure in the solid. The phonons behave as Bose particles and their evolution may be described by the Boltzmann-Peierls equation (BPE), which is an integro-differential equation for the phase density of the phonon gas. The entropy of a Bose gas and the Maximum Entropy Principle (MEP) are used to derive a hierarchy of hyperbolic moment systems.

2. The evolution of transport processes in a gas, whose particles have velocities that are comparable with the speed of light, is described by the relativistic Boltzmann equation. In this study we consider the framework of special relativity and the limiting case of small free flight times of the gas particles. Furthermore we restrict the gas particles to obey Boltzmann statistics, so that local equilibrium is described by the Jüttner phase density. The Maximum Entropy Principle (MEP) serves to derive the relativistic Euler equations for the first five moments of the phase density.

Regarding their mathematical structure, the two examples have many similarities so that we can apply the same numerical method to solve the two described problems. There numerical method is a kinetic scheme which consists of *periods of free flight* and *update times*.

In both examples, the periods of free flight is described by the same collision free kinetic transport equation. The macroscopic fields appear as moments of the phase

density which are formed by integrals over the kinetic variable. In both cases, the moment integrals may be reduced to integrals over the unit sphere.

The update procedure relies in its essential part on the MEP. Thus, we are confronted with the problem whether the MEP exists at all. It was Junk who has pointed out, that the MEP for the Boltzmann equation does not exist, because the moment integrals have an infinite domain. Guided by Junk's seminal contribution, Dreyer, Junk and Kunik studied the Fokker-Planck equation and proved nonexistence also in that case. However, we could prove the existence of the MEP, for the BPE as well as for the ultra-relativistic Euler equations, because both cases lead to moment integrals over the unit sphere.

The described kinetic approach lead to numerical schemes that are first order in time. However, we will describe suitable correction terms that lead to second order schemes.

The first part of this report deals with the BPE. At first we introduce a reduced kinetic equation which has a simpler structure than the BPE. Moreover, if we restrict to the macroscopic 1D case, a further simplification of the kinetic equation is possible. Secondly we give a positive existence result for the MEP. Finally we establish kinetic schemes for the kinetic equation as well as for the hierarchy of hyperbolic moment systems.

In second part of this paper we apply the kinetic approach to the ultra-relativistic Euler equations. We write these in terms of the particle density n, the spatial part of the four-velocity $\mathbf{u}$ and the pressure p.

2 The Boltzmann-Peierls Equation

In this section we use kinetic schemes in order to solve the Boltzmann-Peierls Equations (BPE) as well as the moments systems that are derived by means of the *Maximum Entropy Principle*. Here we present a survey of results that are explained in more detail in [9, 30, 17, 16]. Further results concerning the BPE and its moment systems may be found in [14, 18] and the references therein.

First we give a brief summary on the kinetic theory of heat conduction in 2.1. In 2.2 we introduce a reduced model with a simplified kinetic variable. However, the reduced equation contains all physically relevant information. Afterwards in 2.3 we discuss the strategy of *Extended Thermodynamics* and *Maximum Entropy Principle*. In particular, we derive the moment systems of hyperbolic pde's that approximate the kinetic equation. Finally, in 2.4 we present the kinetic schemes mentioned above. We conclude with some illustrating numerical examples in 2.5.

2.1 The kinetic theory of heat conduction in solids

In 1929, Peierls [35] proposed his celebrated theoretical model to describe transport processes of heat in solids. According to the model the lattice vibrations responsible for the heat transport can be described as an interacting gas of phonons. An overview on phonon theory and its applications is given by Dreyer and Struchtrup in [18].

The BPE is a kinetic equation that describes the evolution of the phase density $f(t, \mathbf{x}, \mathbf{k})$ of a phonon gas. The microscopically three dimensional BPE reads

$$\frac{\partial f}{\partial t} + c k_i \frac{\partial f}{\partial x_i} = Sf, \tag{1}$$

where t, $\mathbf{x} = (x_1, x_2, x_3)$, $\mathbf{k} = (k_1, k_2, k_3)$ denote the time, the space and the wave vector, respectively. The positive constant c is the Debye speed and S abbreviates the collision operator that will be defined below.

The moments of the phase density f reflect the kinetic processes on the scale of continuum physics. The most important moments are the energy density e and the heat flux $\mathbf{Q} = (Q_1, Q_2, Q_3)$ which are defined as

$$e(f) = \hbar c \int\limits_{\mathbb{R}^3} |\mathbf{k}|\, f(\mathbf{k})\, d\mathbf{k}, \quad \mathbf{Q}(f) = \hbar c^2 \int\limits_{\mathbb{R}^3} \mathbf{k} f(\mathbf{k})\, d\mathbf{k}. \tag{2}$$

Since f depends on time and space the moments $e(f)$ and $\mathbf{Q}(f)$ depend on t and $\mathbf{x}$, too.

Phonons are identified as Bose particles, see [35, 18]. Thus, the kinetic entropy density-entropy flux pair $(h, \mathbf{\Phi})$ is given by

$$h(f) = y \int\limits_{\mathbb{R}^3} \left[\left(1 + \frac{f}{y}\right) \ln \left(1 + \frac{f}{y}\right) - \frac{f}{y} \ln \left(\frac{f}{y}\right) \right] d\mathbf{k}, \tag{3}$$

$$\varphi_i(f) = y \int\limits_{\mathbb{R}^3} c \frac{k_i}{|\mathbf{k}|} \left[\left(1 + \frac{f}{y}\right) \ln \left(1 + \frac{f}{y}\right) - \frac{f}{y} \ln \left(\frac{f}{y}\right) \right] d\mathbf{k}, \tag{4}$$

where $y = \frac{3}{8\pi^3}$. The kinetic equation (1) implies the following entropy inequality

$$\frac{\partial h(f)}{\partial t} + \frac{\partial \Phi_j(f)}{\partial x_j} \geq 0. \tag{5}$$

In contrast to ordinary gas atoms, phonons may interact by two different collision processes, called R- and N-processes. N-processes describe phonon-phonon interactions, while R-processes take care of interactions of phonons and lattice impurities. The N-processes conserve energy as well as momentum, while the R-processes conserve only the energy. The Callaway approximation of the collision operator is a suitable simplification of the actual interaction processes (cf. [2, 18]). The Callaway

collision operator is written as the sum of two relaxation operators modelling the R- and N-processes separately. There holds

$$Sf = S_R f + S_N f, \quad S_\alpha f = \frac{1}{\tau_\alpha}\Big(P_\alpha f - f\Big), \quad \alpha \in \Big\{R,\, N\Big\}. \tag{6}$$

The positive constants τ_R and τ_N are the relaxation times, P_R and P_N are two nonlinear projectors. The phase densities $P_R f$ and $P_N f$ are defined as solutions of the two optimization problems

$$h(P_R f) \;=\; \max_{f'} \Big\{ h(f') \,:\, e(f') = e(f) \Big\}, \tag{7}$$

$$h(P_N f) \;=\; \max_{f'} \Big\{ h(f') \,:\, e(f') = e(f),\; \mathbf{Q}(f') = \mathbf{Q}(f) \Big\}. \tag{8}$$

These maximization problems may be solved explicitly. The resulting expressions for P_R and P_N in terms of e and $\mathbf{Q}$ may be found in [18, 30].

2.2 The reduced Boltzmann-Peierls Equation

In this section we recall results from [9, 30] in order to derive a reduced kinetic equation for a reduced phase density. This procedure relies on the observation that for any solution f of (1) there exists a corresponding solution of a reduced equation that determines all physically important moments of f.

For any phase density f depending on the wave vector $\mathbf{k} \in \mathbb{R}^3$ we define the *reduced phase density* φ_f of f depending on a normal vector $\mathbf{n} \in S^2$ by

$$\varphi_f(\mathbf{n}) = \hbar c \int_0^\infty |\mathbf{k}|^3 \, f(|\mathbf{k}|\,\mathbf{n})\, d|\mathbf{k}|, \tag{9}$$

where $\mathbf{n} = (n_1,\, n_2,\, n_3) = \mathbf{k}/|\mathbf{k}|$.

Let m be a homogeneous moment weight of degree 1, i.e. $m(\lambda \mathbf{k}) = \lambda m(\mathbf{k})$ for all $\lambda \geq 0$, and let u be the corresponding moment function. Note that all physically important moments are homogeneous of degree 1.

A straight forward calculation yields

$$u(f) = \hbar c \oint_{S^2} m(\mathbf{n}) \varphi_f(\mathbf{n})\, dS(\mathbf{n}), \tag{10}$$

whereas $dS(\mathbf{n})$ denotes the usual measure on the unit sphere S^2. We conclude that the moment of f is given by a respective moment of it's reduced phase density φ_f. In particular we find $e(f) = e(\varphi_f)$ and $\mathbf{Q}(f) = \mathbf{Q}(\varphi_f)$ with

$$e(\varphi) = \oint_{S^2} \varphi(\mathbf{n})\, dS(\mathbf{n}),\; \mathbf{Q}(\varphi) = c \oint_{S^2} \mathbf{n} \varphi(\mathbf{n})\, dS(\mathbf{n}). \tag{11}$$

Furthermore, we introduce an entropy density-entropy flux pair $(h,\, \mathbf{\Phi})$ for reduced phase densities by

$$h(\varphi) = \mu \oint\limits_{S^2} \varphi^{\frac{3}{4}}(\mathbf{n})\, dS(\mathbf{n}), \quad \Phi_i(\varphi) = \mu\, c \oint\limits_{S^2} n_i\, \varphi^{\frac{3}{4}}(\mathbf{n})\, dS(\mathbf{n}), \tag{12}$$

where μ is a given constant. We summarize the main results in the following theorem.

Theorem 2.1 *1. There exist two operators Θ_R and Θ_N so that*

$$\varphi_{(P_\alpha f)} = \Theta_\alpha(\varphi_f) \quad \textit{for} \quad \alpha \in \{R,\, N\}. \tag{13}$$

2. If f is a solution of the BPE, then its reduced phase density φ_f is a solution of the following reduced BPE

$$\frac{\partial\, \varphi}{\partial\, t} + c n_i \frac{\partial\, \varphi}{\partial\, x_i} = \Psi \varphi, \tag{14}$$

where $\Psi = \Psi_R + \Psi_N$ and $\Psi_\alpha \varphi = \frac{1}{\tau_\alpha}(\Theta_\alpha \varphi - \varphi)$.

3. Θ_R and Θ_N have similar properties as P_R and P_N, i.e.

$$h(\Theta_R \varphi) \;=\; \max_{\varphi'} \Big\{ h(\varphi') \,:\, e(\varphi') = e(\varphi) \Big\}, \tag{15}$$

$$h(\Theta_N \varphi) \;=\; \max_{\varphi'} \Big\{ h(\varphi') \,:\, e(\varphi') = e(\varphi),\, \mathbf{Q}(\varphi') = \mathbf{Q}(\varphi) \Big\}. \tag{16}$$

4. There holds

$$\Theta_R \varphi = \frac{e}{4\pi},\; \Theta_N \varphi = \frac{3e(4-F)^3}{4\pi F \left(1 - \frac{F\, \mathbf{n}\cdot\mathbf{Q}}{4\, c\, e}\right)^4},\; F = \frac{6}{1 + \sqrt{1 - \frac{3}{4}\left(\frac{|\mathbf{Q}|}{c\, e}\right)^2}}. \tag{17}$$

5. The reduced BPE implies the entropy inequality

$$\frac{\partial\, h(\varphi)}{\partial\, t} + \frac{\partial\, \Phi_i(\varphi)}{\partial\, x_i} \geq 0. \tag{18}$$

6. The reduced BPE leads to an hierarchy of balance laws. For any vector of moment weights $\vec{m}(\mathbf{n})$ we obtain

$$\frac{\partial\, \vec{u}(\varphi)}{\partial\, t} + \frac{\partial\, \vec{F}_i(\varphi)}{\partial\, x_i} = \vec{\Pi}(\varphi), \tag{19}$$

where

$$\vec{u}(\varphi) \;=\; \oint\limits_{S^2} \vec{m}(\mathbf{n}) \varphi(\mathbf{n})\, dS(\mathbf{n}), \tag{20}$$

$$\vec{F}_i(\varphi) \;=\; \oint\limits_{S^2} c n_i \vec{m}(\mathbf{n}) \varphi(\mathbf{n})\, dS(\mathbf{n}), \tag{21}$$

$$\vec{\Pi}(\varphi) \;=\; \oint\limits_{S^2} \vec{m}(\mathbf{n}) \big(\Psi \varphi\big)(\mathbf{n})\, dS(\mathbf{n}), \tag{22}$$

denote the densities, the fluxes and the productions, respectively.

2.2.1 One-dimensional Reduced Kinetic Equation

To conclude this section we summarize results from [30] that allow a further simplification of the reduced BPE. In the macroscopically one dimensional case we have $\mathbf{x} = (x, 0, 0)$ and $\mathbf{Q} = (Q, 0, 0)$. We introduce the new variables $-1 \leq \xi \leq 1$, $0 \leq \vartheta \leq 2\pi$ by

$$n_1 = \xi\,, \qquad n_2 = \sqrt{1-\xi^2}\sin\vartheta\,, \qquad n_3 = \sqrt{1-\xi^2}\cos\vartheta\,, \tag{23}$$

with the surface element $dS(\mathbf{n}) = d\xi d\vartheta$. Furthermore we eliminate the angle ϑ by setting

$$\varphi(t, x, \xi) = \int_0^{2\pi} \varphi(t, x, 0, 0, \mathbf{n})\, d\vartheta. \tag{24}$$

The reduced BPE (14) then further reduces to

$$\frac{\partial\varphi}{\partial t} + c\,\xi\,\frac{\partial\varphi}{\partial x} = \frac{1}{\tau_R}\left(\Theta_R\varphi - \varphi\right) + \frac{1}{\tau_N}\left(\Theta_N\varphi - \varphi\right), \tag{25}$$

where $\Theta_R\varphi$ and $\Theta_N\varphi$ are given by expressions similar to (17).

2.3 The Maximum Entropy Principle

2.3.1 The strategy of Extended Thermodynamics

The objective of *Extended Thermodynamics* is to solve initial and boundary value problems for truncated moment systems instead of solving the kinetic equation. To this end only the first N equations of the infinite hierarchy of moment equation are used, and the *Maximum Entropy Principle* (MEP) serves to close the truncated system.

For the formulation of the MEP we start with a fixed N-dimensional vector $\vec{m} = \vec{m}(\mathbf{n})$ of moment weights. The vector $\vec{m}$ induces a vector $\vec{u}$ of densities, cf. (20). In the following we call the pair $(\vec{m}, \vec{u})$ a *moment pair* of dimension N. The MEP corresponding to $(\vec{m}, \vec{u})$ can be formulated as follows.

For any given phase density φ we seek a phase density φ_M that maximizes the entropy, i.e.

$$h\left(\varphi_M\right) = \max_{\varphi'}\ \left\{\ h\left(\varphi'\right)\ :\ \vec{u}\left(\varphi'\right) = \vec{u}\left(\varphi\right)\ \right\}. \tag{26}$$

In order to indicate that φ_M obviously depends on φ, we write $\varphi_M = \Theta_M\varphi$. The MEP assumes, that for any reasonable phase density φ there always exists a phase density $\varphi_M = \Theta_M\varphi$ that maximizes the entropy according to (26). Thus, the MEP ends up with an operator Θ_M with the following properties

1. Θ_M is a nonlinear projector, i.e. $\Theta_M^2 = \Theta_M$.

2. $\Theta_M f$ depends only on the moments $\vec{u}(\varphi)$, i.e. $\vec{u}(\varphi_1) = \vec{u}(\varphi_2)$ implies $\Theta_M \varphi_1 = \Theta_M \varphi_2$.

We call the operator Θ_M the *MEP projector* corresponding to the moment pair $(\vec{m}, \vec{u})$.

We mention that, according to (15) and (16), the operators Θ_R and Θ_N appearing in the reduced collision operation Ψ are also MEP projectors.

Next we consider the closure problem of *Extended Thermodynamics*. We start with a finite number of balance equations derived from the kinetic equation, cf. (19). As before we denote the corresponding vectors of densities and fluxes by $\vec{u}$ and $\vec{F}_j$, respectively. The densities are now considered as the independent variables. Since in general the fluxes $\vec{F}_j$ do not depend on the densities $\vec{u}$, there arises the so called closure problem. The closure problem is solved by a reasonable ansatz that provides the fluxes and the productions as functions of the densities.

A very popular closure ansatz in *Extended Thermodynamics* is the MEP leading to the so called MEP moment system, which is achieved from (14) by a formal replacement of the phase density φ by the MEP density $\Theta_M \varphi$:

$$\frac{\partial \vec{u}(\Theta_M \varphi)}{\partial t} + \frac{\partial \vec{F}_j(\Theta_M \varphi)}{\partial x_j} = \vec{u}(\Psi \Theta_M \varphi). \tag{27}$$

Since $\Theta_M \varphi$ depends on φ via the densities $\vec{u}$, the system (27) is in fact a closed system with respect to the variables $\vec{u}$. The resulting system of PDE's is symmetric hyperbolic. For further details we refer to the standard textbook on *Rational Extended Thermodynamics* by Müller/Ruggeri ([33]) and to [9].

The existence of the MEP projector is a nontrivial and subtle problem, because there are counterexamples in which the MEP fails. Junk has observed, that for the Boltzmann Equation the corresponding MEP density does not exist in general. A detailed discussion of this problem may be found in [24, 25, 11].

However, in the case of the reduced BPE these problems do not arise. This topic will be discussed in the next subsection.

2.3.2 The MEP and the reduced equation

We apply the MEP to the reduced kinetic equation and to the entropy (12). In particular, we give a positive existence result for MEP projectors Θ_M.

Let $(\vec{m}, \vec{u})$ be a moment pair of dimension N. We call the pair $(\vec{m}, \vec{u})$ *admissible*, if (i) the energy density e is among the components of $\vec{u}$ and if (ii) the components of $\vec{m}$ are smooth (at least C^3). In the following, we consider exclusively admissible pairs $(\vec{m}, \vec{u})$.

For $r \in \{1, \infty\}$ we define

$$L^r_+(S^2) \;=\; \Big\{ \varphi \in L^r(S^2) \;:\; \exists\, \delta = \delta(\varphi) > 0 \text{ with } \varphi \geq \delta \text{ a.e.} \Big\}. \tag{28}$$

For given $\varphi \in L^1_+(S^2)$ the MEP leads to the following optimization problem with constraints.

Problem 2.2

$$h(\varphi_M) \;=\; \max_{\varphi'} \Big\{ h(\varphi') \;:\; \varphi' \in L^1_+(S^2),\; \vec{u}(\varphi') = \vec{u}(\varphi) \Big\}. \tag{29}$$

Next we introduce the conjugate functional $h^\star$ of the entropy h, that reads

$$h^\star(\psi) \;=\; -\frac{1}{3}\left(\frac{3}{4}\mu\right)^4 \int_{S^2} \psi^{-3}(\mathbf{n})\, d\mathbf{n}. \tag{30}$$

Note that $h^\star$ is well defined for all $\psi \in L^\infty_+(S^2)$. Using this functional $h^\star$ we formulate the following dual problem of 2.2, namely

Problem 2.3

$$\tilde{h}(\vec{\Lambda}_M) \;=\; \min_{\vec{\Lambda}} \Big\{ \tilde{h}(\vec{\Lambda}) \;:\; \vec{\Lambda} \in D_M \Big\}, \tag{31}$$

$$D_M \;:=\; \Big\{ \vec{\Lambda} \in \mathbb{R}^n \;:\; \vec{\Lambda} \cdot \vec{m} \in L^\infty_+(S^2) \Big\}, \tag{32}$$

$$\tilde{h}(\vec{\Lambda}) \;=\; -h^\star\Big(\vec{\Lambda} \cdot \vec{m}\Big) + \vec{u}(\varphi_0) \cdot \vec{\Lambda}, \tag{33}$$

which is an optimization problem without constraints. There is a close relation between the Problems 2.2 and 2.3. In particular, the solution $\vec{\Lambda}_M$ of Problem 2.3 are the Lagrange multipliers corresponding to the solution φ_M of Problem 2.2. The main results concerning the MEP are summarized in the following theorem.

Theorem 2.4 *For any $\varphi \in L^1_+(S^2)$ there holds*

1. *There exists a unique solution φ_M of problem 2.2.*
2. *There exists a unique solution $\vec{\Lambda}_M$ of problem 2.3.*
3. *There holds the identity*

$$\varphi_M \;=\; \left(\frac{3}{4}\frac{\mu}{\vec{\Lambda}_M \cdot \vec{m}}\right)^4. \tag{34}$$

The proof of a similar result for two dimensions is contained in [9].

2.4 Kinetic schemes

2.4.1 Kinetic solutions of the kinetic equation

In this section we derive kinetic schemes that allow the construction of approximate solutions of (14) in the time interval $[0, \infty)$.

The solution of the Cauchy problem of the collisionless kinetic equation

$$\frac{\partial \varphi}{\partial t} + cn_i \frac{\partial \varphi}{\partial x_i} = 0, \tag{35}$$

is given by the *free transport group* $T(t)$ acting on phase densities φ depending on $\mathbf{x}$ and $\mathbf{n}$ according to

$$\Big(T(t)\varphi\Big)(\mathbf{x}, \mathbf{n}) := \varphi(\mathbf{x} - ct\mathbf{n}, \mathbf{n}). \tag{36}$$

In particular, $T(t)\varphi^0$ is a solution of (35) with initial data φ^0.

The solution of the corresponding Cauchy problem for the reduced BPE (14) can be represented by means of Duhamel's principle as

$$\varphi(t) = T(t)\varphi^0 + \int_0^t T(t-s)\big(\Psi_R\varphi(s) + \Psi_N\varphi(s)\big)\, ds. \tag{37}$$

Note that for any t the function $\varphi(t)$ is a phase density depending on $\mathbf{x}$ and $\mathbf{n}$. Obviously, the formula (37) is not explicit in $\varphi(t)$. In order to find approximate solutions, we shall replace the integrals in (37) by Riemann sums. If we introduce a small parameter $\tilde{\tau} > 0$, we find

$$\varphi(t) \simeq T(t)\varphi^0 + \sum_{k\,:\,0 \le k\,\tilde{\tau} < t} \tilde{\tau}\, T(t - k\tilde{\tau})\big(\Psi_R\varphi(k\tilde{\tau}) + \Psi_N\varphi(k\tilde{\tau})\big). \tag{38}$$

This approximate representation of solutions of (14) immediately gives rises to an explicit semidiscret kinetic scheme. Using the abbreviations

$$\varphi_{k\pm} = \lim_{t \downarrow 0} \varphi(k\tilde{\tau} \pm t) \quad \text{for} \quad k \ge 0, \tag{39}$$

and $\varphi_{0-} = \varphi^0$, we find by a straight forward calculation, that (38) with equality sign is equivalent to

$$\varphi(k\tilde{\tau} + t) = T(t)\varphi_{k+}, \quad 0 < t < \tilde{\tau}, \tag{40}$$

$$\varphi_{k+} = \frac{\tilde{\tau}}{\tau_R}\Theta_R\varphi_{k-} + \frac{\tilde{\tau}}{\tau_N}\Theta_N\varphi_{k-} + \Big(1 - \frac{\tilde{\tau}}{\tau_R} - \frac{\tilde{\tau}}{\tau_N}\Big)\varphi_{k-}. \tag{41}$$

The time intervals $(k\tilde{\tau},\, k\tilde{\tau} + \tilde{\tau})$ are called *transport intervals*, whereas the multiples of $\tilde{\tau}$ are called *update times*.

For any strictly positive initial datum φ^0 and sufficiently small parameter $\tilde{\tau}$, the kinetic scheme (40)-(41) defines an approximate solution φ of (14) with the following properties.

Lemma 2.5

1. *$\varphi(t)$ is strictly positive for all t and there exist the left-hand and right-hand limits at the update times.*

2. *φ satisfies exactly the conservation of energy, that is*

$$\frac{\partial\, e(\varphi)}{\partial\, t} + \frac{\partial\, Q_i(\varphi)}{\partial\, x_i} \;=\; 0. \tag{42}$$

3. *The entropy production is nonnegative, i.e.*

$$\frac{\partial\, h(\varphi)}{\partial\, t} + \frac{\partial\, \Phi_i(\varphi)}{\partial\, x_i} \;\geq\; 0. \tag{43}$$

The equation (42) *and the inequality* (43) *are satisfied in the sense of distributions.*

For further details again we refer to [9].

2.4.2 Kinetic solution of the MEP moment systems

In this section we shall briefly describe how kinetic schemes can be used in order to solve moment systems of the reduced kinetic equation that are derived by means of the MEP. It will turn out, that there is a close relationship between kinetic schemes for the kinetic equation and kinetic schemes for its moment systems. A more detailed discussion is contained in [9].

In the following we consider an admissible moment pair $(\vec{u},\, \vec{m})$ together with the resulting MEP projector Θ_M (cf. Subsection 2.3). The moment system corresponding to $\vec{u}$ is given by

$$\frac{\partial\, \vec{u}(\Theta_M\varphi)}{\partial\, t} + \frac{\partial\, \vec{F}_j(\Theta_M\varphi)}{\partial\, x_j} \;=\; \vec{u}(\Psi\Theta_M\varphi). \tag{44}$$

The standard kinetic approach of the Cauchy problem for this moment system can be summarized as follows.

1. We start with initial data of the form $\Theta_M\varphi^0$ that correspond to the given macroscopic initial data $\vec{u}^0$, i.e. $\vec{u}^0 = \vec{u}(\Theta_M\varphi^0)$.

2. For a small but fixed time τ_M we solve the kinetic equation (14) for in the time interval $[0,\, \tau_M]$, at least approximately.

3. The resulting phase density will be used to calculate the moments $\vec{u}$.

4. At the time τ_M the phase density $\varphi(\tau_M)$ will be replaced by the MEP phase density $\Theta_M\varphi(\tau_M)$ and we restart the scheme.

Kinetic schemes of this kind are well known and studied by many authors for moment systems relying on various kinetic equations (see [10, 12, 13, 24, 36] for moment systems of the Boltzmann Equation, [14, 15] for a moment system of the BPE).

In view of this standard approach we consider the following kinetic equation

$$\frac{\partial \varphi}{\partial t} + cn_i \frac{\partial \varphi}{\partial x_i} = \Psi_R \varphi + \Psi_N \varphi + \Psi_M \varphi \tag{45}$$

The newly introduced quantity is

$$\Psi_M \varphi \ = \frac{1}{\tau_M}\Big(\Theta_M \varphi - \varphi\Big) \tag{46}$$

that is again a relaxation operator with an artificial relaxation time τ_M.

If we apply the moment maps $\vec{u}$ to (45), we formally obtain for the limiting case $\tau_M \to 0$ the system (44). We can thus interpret equation (45) as a kinetic approximation of the moment system (44).

Next we apply the approach from above to the kinetic equation (45). There result the following kinetic scheme

$$\varphi(k\tilde{\tau} + t) \ = \ T(t)\varphi_{k+}, \quad 0 < t < \tilde{\tau}, \tag{47}$$

$$\begin{aligned} \varphi_{k+} \ = \ & \frac{\tilde{\tau}}{\tau_R}\Theta_R \varphi_{k-} + \frac{\tilde{\tau}}{\tau_N}\Theta_N \varphi_{k-} + \frac{\tilde{\tau}}{\tau_M}\Theta_M \varphi_{k-} + \\ & \Big(1 - \frac{\tilde{\tau}}{\tau_R} - \frac{\tilde{\tau}}{\tau_N} - \frac{\tilde{\tau}}{\tau_M}\Big)\varphi_{k-}. \end{aligned} \tag{48}$$

This scheme differs from (40)-(41) just in the update rule (48). However, all assertions of Lemma 2.5 remain valid.

2.4.3 Fully Discretized First Order Scheme

In order to get a fully discretized piecewise constant solution of the reduced BPE (25), we first define a grid in the reduced phase-space consisting of cells $C_{i,j} = I_i \times J_j$ centered around $(x_i = i\Delta x,\ \xi_j = j\Delta\xi)$,

$$C_{i,j} = \left\{ (x,\xi) \in \mathbb{R}^2 \ \middle| \ |x - x_i| \le \frac{\Delta x}{2} \ , \quad |\xi - \xi_j| \le \frac{\Delta \xi}{2} \right\},$$

where $\Delta x = x_{i+\frac{1}{2}} - x_{i-\frac{1}{2}}$ and $\Delta\xi = \xi_{j+\frac{1}{2}} - \xi_{j-\frac{1}{2}}$. The cell-average of φ at time $t = t_n$ over the cell $C_{i,j}$ is given by

$$\varphi_{i,j}^n = \frac{1}{\Delta x \Delta \xi} \int\limits_{x_{i-\frac{1}{2}}}^{x_{i+\frac{1}{2}}} \int\limits_{\xi_{j-\frac{1}{2}}}^{\xi_{j+\frac{1}{2}}} \varphi(t,x,\xi)\, d\xi dx \, . \tag{49}$$

With the characteristic function $\chi_{i,j}(x,\xi)$ of the cell $C_{i,j}$ we can write the desired piecewise constant phase density in the form $\sum \varphi^n_{i,j}\chi_{i,j}(x,\xi)$.

Integrating (40)-(41) over $\left[x_{i-\frac{1}{2}}, x_{i+\frac{1}{2}}\right] \times \left[\xi_{j-\frac{1}{2}}, \xi_{j+\frac{1}{2}}\right]$ and dividing by $\Delta x \Delta \xi$, we get for a time step $\tilde{\tau} = \Delta t$

$$\varphi^{n+1}_{i,j} = \varphi^n_{i,j} - \lambda\left(\mathcal{F}^n_{i+\frac{1}{2},j} - \mathcal{F}^n_{i-\frac{1}{2},j}\right) + \Delta t\, \mathcal{S}^n_{i,j} + O(\Delta t)^2\,, \tag{50}$$

where $\lambda = \frac{\Delta t}{\Delta x}$, and for the CFL condition $\Delta t \leq \frac{\Delta x}{2}$ we have

$$\mathcal{S}^n_{i,j} = \sum_{\alpha \in R,N} \frac{1}{\tau_\alpha}\left(\Theta_\alpha \varphi^n_{i,j} - \varphi^n_{i,j}\right)\,, \tag{51}$$

$$\mathcal{F}^n_{i+\frac{1}{2},j} = \frac{c}{2}\left(\xi_j \varphi^n_{i,j} + \xi_j \varphi^n_{i+1,j} - |\xi_j| \Delta \varphi^n_{i,j}\right)\,, \tag{52}$$

where $\Delta\varphi^n_{i,j} = \varphi^n_{i+1,j} - \varphi^n_{i,j}$. In order to get the average values of the moments from this discrete phase density at any time t_n in each cell I_i we use the Riemann sums as

$$e^n_i = \Delta\xi \sum_{j=1}^{N_\xi} \varphi^n_{i,j}, \quad Q^n_i = c\Delta\xi \sum_{j=1}^{N_\xi} \xi_j \varphi^n_{i,j}, \quad N^n_i = \Delta\xi \sum_{j=1}^{N_\xi} \xi_j^2 \varphi^n_{i,j}\,, \tag{53}$$

where N_ξ is the number of elements in the interval $-1 \leq \xi \leq 1$.

2.4.4 Second Order Extension of the Scheme

For the second order accuracy in space and time we have the following three steps.

(I) Data Reconstruction: Starting with a piecewise-constant solution in time and phase-space, $\sum \varphi^n_{i,j}\chi_i(x)$, one reconstruct a piecewise linear (MUSCL-type) approximation in space, namely

$$\varphi^n_j(x) = \sum \left[\varphi^n_{i,j} + \varphi^x_{i,j}\frac{(x - x_i)}{\Delta x}\right] \chi_{i,j}(x,\xi)\,. \tag{54}$$

Here, $\varphi^x_{i,j}$ abbreviates a first order discrete slope.

The extreme points $x = 0$ and $x = \Delta x$, in local coordinates correspond to the intercell boundaries in general coordinates $x_{i-\frac{1}{2}}$ and $x_{i+\frac{1}{2}}$, respectively, see Figure 1. The values of $\varphi_{i,j}$ at the extreme points are

$$\varphi^L_{i,j} = \varphi^n_{i,j} - \frac{1}{2}\varphi^x_{i,j}\,, \quad \varphi^R_{i,j} = \varphi^n_{i,j} + \frac{1}{2}\varphi^x_{i,j}\,, \tag{55}$$

and are usually called *boundary extrapolated values*. A possible computation of these slopes, which results in an overall non-oscillatory schemes (consult [39]), is given by

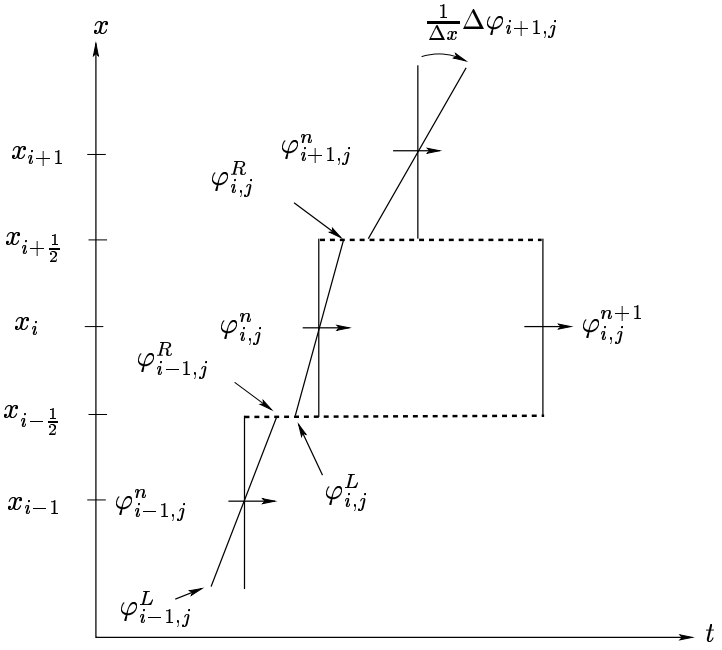

Figure 1: Second order reconstruction

family of *discrete derivatives* parameterized with $1 \leq \theta \leq 2$, i.e., for any grid function $\varphi_{i,j}$ we set

$$\varphi^x_{i,j} = MM\left(\theta\Delta\varphi_{i+\frac{1}{2},j}, \frac{\theta}{2}(\Delta\varphi_{i-\frac{1}{2},j} + \Delta\varphi_{i+\frac{1}{2},j}), \theta\Delta\varphi_{i-\frac{1}{2}}, j\right) .$$

Here, Δ denotes the forward differencing, $\Delta\varphi_{i+\frac{1}{2},j} = \varphi_{i+1,j} - \varphi_{i,j}$, and MM denotes the min-mod nonlinear limiter

$$MM\{x_1, x_2, ...\} = \begin{cases} \min_i\{x_i\} & \text{if } x_i > 0 \quad \forall i\,, \\ \max_i\{x_i\} & \text{if } x_i < 0 \quad \forall i\,, \\ 0 & \text{otherwise}\,. \end{cases} \tag{56}$$

The interpolant (54), is then evolved exactly in time and projected on the cell-averages at the next time step.

(II) Evolution: For each cell I_i, the boundary extrapolated values $\varphi^L_{i,j}$, $\varphi^R_{i,j}$ in (55) are evolved for a time $\frac{1}{2}\Delta t$ by

$$\begin{aligned} \hat{\varphi}^L_{i,j} &= \varphi^L_{i,j} - \frac{\lambda}{2}\left[\mathcal{F}^R_{i,j} - \mathcal{F}^L_{i,j}\right] + \frac{\Delta t}{2}\mathcal{S}^n_{i,j}\,, \\ \hat{\varphi}^R_{i,j} &= \varphi^R_{i,j} - \frac{\lambda}{2}\left[\mathcal{F}^R_{i,j} - \mathcal{F}^L_{i,j}\right] + \frac{\Delta t}{2}\mathcal{S}^n_{i,j}\,, \end{aligned} \tag{57}$$

where $\mathcal{F}^L_{i,j} = c\xi_j\varphi^L_{i,j}$ and $\mathcal{F}^R_{i,j} = c\xi_j\varphi^R_{i,j}$. Also to calculate source term at half time step we use

$$\hat{\varphi}_{i,j} = \varphi^n_{i,j} - \frac{\lambda}{2}\left[\mathcal{F}^n_{i+1,j} - \mathcal{F}^n_{i,j}\right] + \frac{\Delta t}{2}\mathcal{S}^n_{i,j}\,, \tag{58}$$

where $\mathcal{F}^n_{i,j} = c\xi_j\varphi^n_{i,j}$ and

$$\hat{e}_i = \Delta\xi \sum_{j=1}^{N_\xi} \hat{\varphi}_{i,j}, \quad \hat{Q}_i = c\Delta\xi \sum_{j=1}^{N_\xi} \xi_j \hat{\varphi}_{i,j}\,. \tag{59}$$

(III): Finally we use the conservative formula (50) in order to get the discrete phase density at next time step

$$\varphi^{n+1}_{i,j} = \varphi^n_{i,j} - \lambda\left(\mathcal{F}^{n+\frac{1}{2}}_{i+\frac{1}{2},j} - \mathcal{F}^{n+\frac{1}{2}}_{i-\frac{1}{2},j}\right) + \sum_{\alpha\in R,N} \frac{\Delta t}{\tau_\alpha}\left(\Theta_\alpha\hat{\varphi}_{i,j} - \hat{\varphi}_{i,j}\right), \tag{60}$$

where the numerical fluxes are defined by

$$\mathcal{F}^{n+\frac{1}{2}}_{i+\frac{1}{2},j} = \frac{c}{2}\left[\xi_j\hat{\varphi}^R_{i,j} + \xi_j\hat{\varphi}^L_{i+1,j} - |\xi_j|(\hat{\varphi}^L_{i+1,j} - \hat{\varphi}^R_{i,j})\right]\,. \tag{61}$$

2.5 Numerical Examples

The results of the preceding section shall be illustrated by some numerical examples.

2.5.1 Example 1: The phenomenon of second sound

The first two examples we have taken from [9] allthough there we rely on the microscopic two dimensional version of the BPE. However, the qualitative behavior does not depend on the number of microscopic dimensions. For both examples we assume that $\tau_R = \infty$. Further we assume that the phase density only depends on x_1. In order to simulate interesting phenomena, we consider the following macroscopic initial data for energy density e and the momentum density Q.

$$\begin{aligned} e^0(x_1) &= \begin{cases} 1.5 & \text{if} \quad |x_1| \le 0.01 \\ 1.0 & \text{if} \quad |x_1| > 0.01 \end{cases}, \\ Q_1(x_1) &= 0. \end{aligned}$$

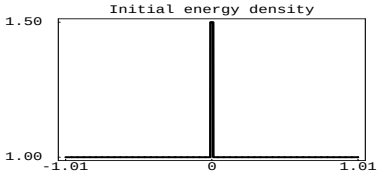

For the details of discretization we refer to [9].

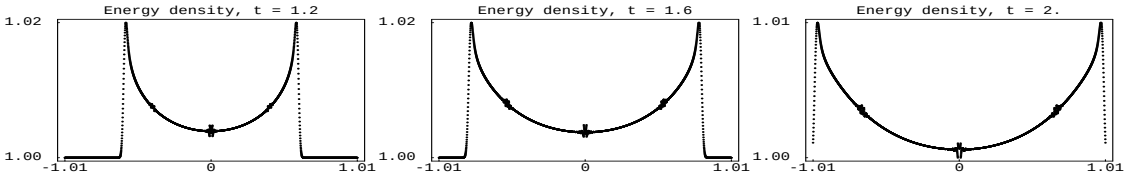

Figure 2: Example 1. Evolution of the energy pulse for $\tau_N = 2.0$

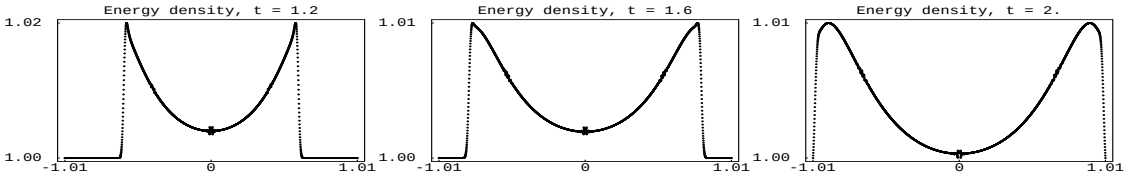

Figure 3: Example 1. Evolution of the energy pulse for $\tau_N = 1.0$

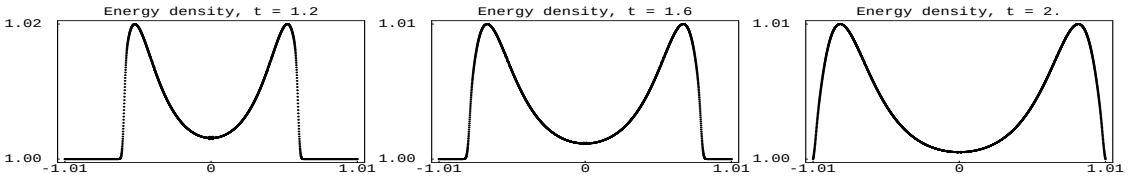

Figure 4: Example 1. Evolution of the energy pulse for $\tau_N = 0.5$

We study the evolution of the initial energy pulse according to different values of τ_N ($\tau_N = 2.$, $\tau_N = 1.$ and $\tau_N = 0.5$). The Figures 2-4 show the spatial dependence of the energy density at different times ($t = 1.2$, $t = 1.6$ and $t = 2.0$). According to [18] we can interpret the results as follows. For large values of τ_N, as in Figure 2, the pulse is ballistic and its fronts move with the Debye speed c to the left and to the right. Figure 4 illustrates the case of small τ_N. Here, the shape of the pulse reflects the characteristic behaviour of the so called second sound, that propagates with a speed less than c. In Figure 3 we observe a transition regime. The pulse starts as a ballistic pulse. After about 1.6 time units it changes its shape and becomes second sound.

2.5.2 Example 2: Kinetic equation versus MEP moment systems

This example illustrates the relationship between solutions of the kinetic equation and solutions of the moment systems. The initial data are the same as in the first example, the relaxation time τ_N is set to 0.7. The energy density corresponding to the reduced BPE is depicted in Figure 5, whereas Figure 6 show the evolution of the initial energy pulse according to various moment systems. We mention, that the moment system of order n consists of $2n + 1$ independent balance equations. For the details we refer to [9]. The Figures 5 and 6 reveal, that moment systems

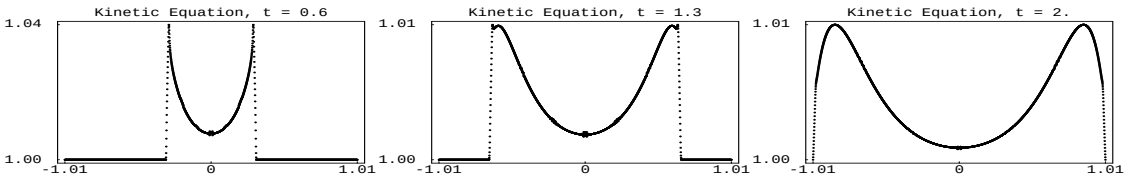

Figure 5: Example 2. Evolution of the energy pulse according to the kinetic equation

with a small number of moments produce quite bad approximations. However, the results become better if the number of moments is increased. Finally we have a

good correspondence of the kinetic equation and of the moment system of order 40 in Figure 6. Furthermore, the Figures exhibit, how the number of appearing waves increases with the order of the moment system. Finally we mention, that

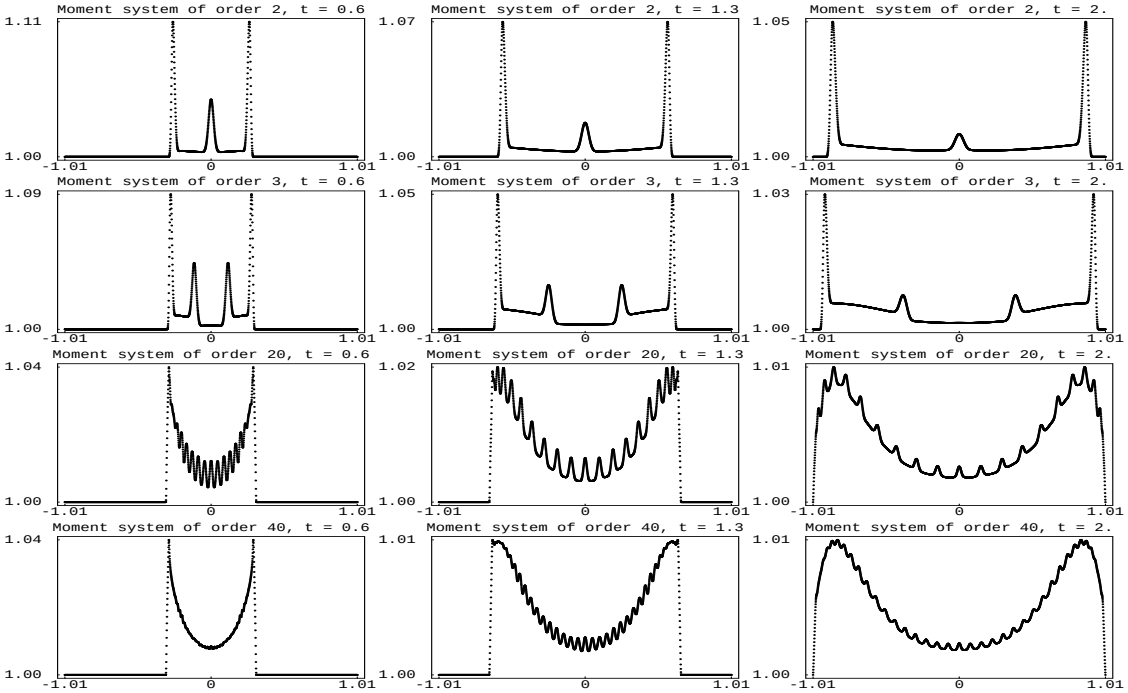

Figure 6: Example 2. Evolution of the energy pulse according to various moment systems

the numerical effort for calculating the MEP projectors Θ_M increases tremendously with the number of moments. A detailed discussion of this problem is contained in [9].

2.5.3 Example 3: Two Interacting Heat Pulses

This test problem demonstrates the interaction of two heat pulses, which leads to a large increase of the energy density at the collision point during a short time interval. The initial data are

$$e(0,x) = \begin{cases} 1\,, & x \le 0.3 \\ 2\,, & 0.3 \le x \le 0.4 \\ 1\,, & 0.4 \le x \le 0.6 \\ 2\,, & 0.6 \le x \le 0.7 \\ 1\,, & x \le 1.0 \end{cases}, \quad Q(0,x) = \begin{cases} 0\,, & x \le 0.3 \\ 1\,, & 0.3 \le x \le 0.4 \\ 0\,, & 0.4 \le x \le 0.6 \\ -1\,, & 0.6 \le x \le 0.7 \\ 0\,, & x \le 1.0 \end{cases}. \tag{62}$$

We solve the BPE for the above problem at time $t = 0.2$ for two values of τ_N, i.e., $\tau_N = 1$ and $\tau_N = 0.1$, while $\tau_R = 1.0$. Figure 7 shows the results. From the comparison of the initial and final curves of energy density, we observe a large increase of the energy density e at the collision point $x = 0.5$. We have also compared

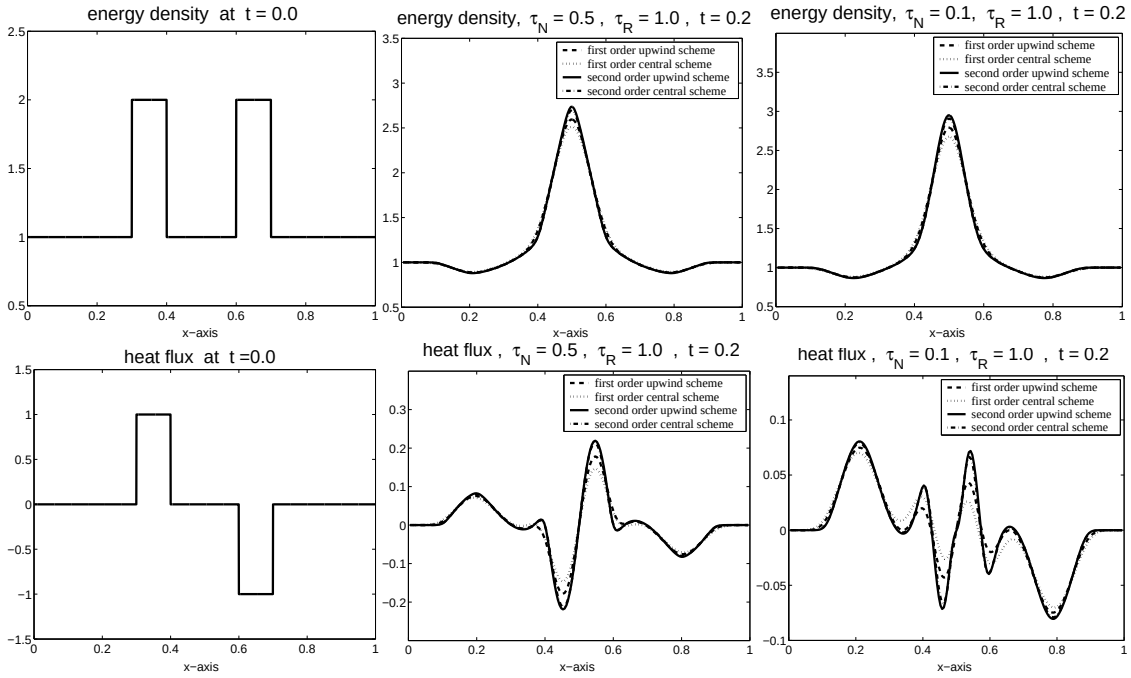

Figure 7: Example 3: Evolution of energy and heat flux.

our results from the kinetic scheme with central schemes of Nessyahu and Tadmor, see [34, 23].

2.5.4 Example 4: Heat Pulse in 2D

In this example we solve a two-dimensional hyperbolic moment system. We consider a two-dimensional energy pulse inside a square box of sides length 0.02 with outflow boundaries. Initially the heat fluxes are zero. The energy density is 1.5 inside a small square box of sides length 0.02 in the center of the large box, while energy density is unity elsewhere. The results are shown at $t = 1.2$ in Figure 8. In all the results we have used 200×200 mesh points. We take $\tau_R = \infty$.

2.5.5 Example 5: Explosion in a Box.

Here we also solve a two-dimensional hyperbolic moment system. We consider a two-dimensional energy pulse inside a square box of sides length 2.0, with periodic boundaries. Initially the heat fluxes are zero. The energy density is 2.0 inside a small square box of sides length 0.5 in the center of the large box, while energy density is unity elsewhere. The results are shown in Figures 9 at $t = 0.5$, $t = 1.5$ and $t = 2.0$. In all the results we have used 300×300 mesh points. We take $\tau_R = \infty$.

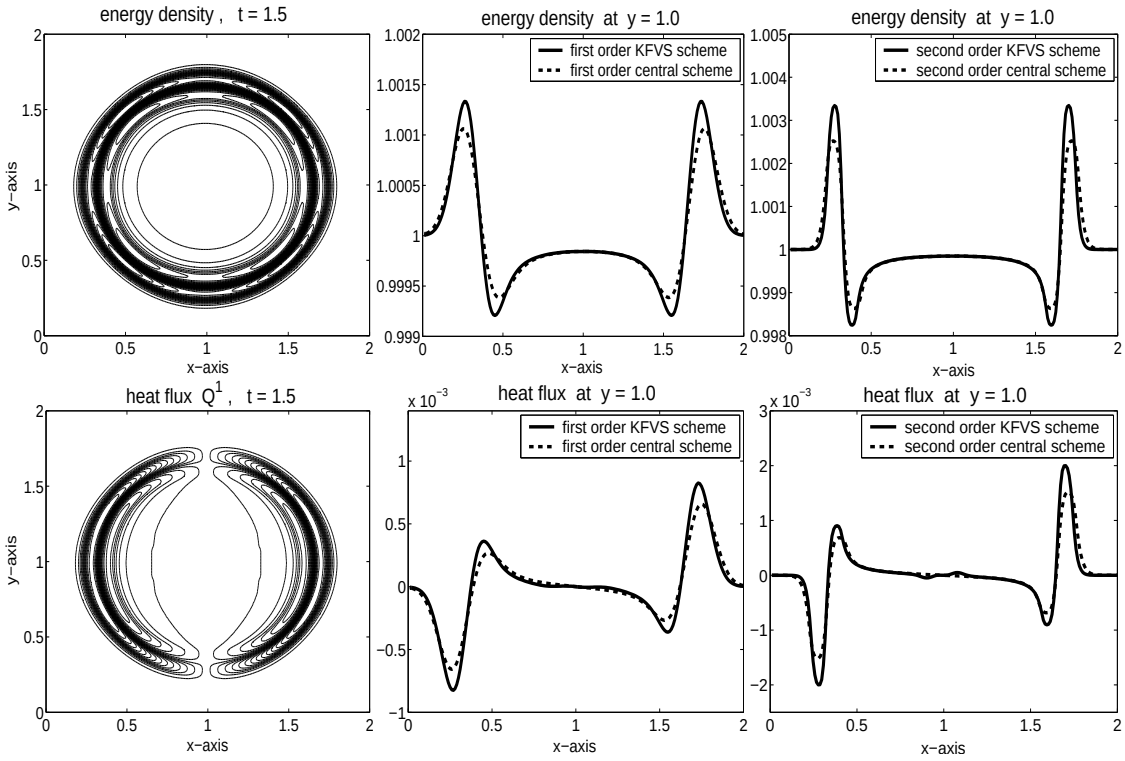

Figure 8: Example 4: Evolution of energy density and heat flux in 2D.

3 Part II: Relativistic Euler Equations

3.1 Introduction

We consider gas flows with thermal and macroscopic velocities that both are comparable with the speed of light. In this case, space and time are coupled and the relativistic Euler equations of gas dynamics become more complicated as compared to the classical ones. However, in some fixed reference frame it is still possible to write the relativistic Euler equations as a first order hyperbolic system.

Relativistic gas dynamics plays an important role in areas of astrophysics, high energy particle beams, high energy nuclear collisions, and free-electron laser technology. Here we consider exclusively the ultra-relativistic limit within the framework of special relativity.

Kinetic approaches to solve the classical Euler equations of gas dynamics were successfully applied to several initial- and boundary value problems, see for example Reitz [38], Deshpande [7, 8], Xu [41, 42], Dreyer and Kunik [12], Dreyer, Herrmann, Kunik [10], and Qamar [37]. Some interesting links between the Euler system and the so called kinetic BGK-model, which was introduced by Bhatnagar, Gross and Krook [1], are discussed in the textbooks by Cercignani [3] as well as by Godlewski and Raviart [22].

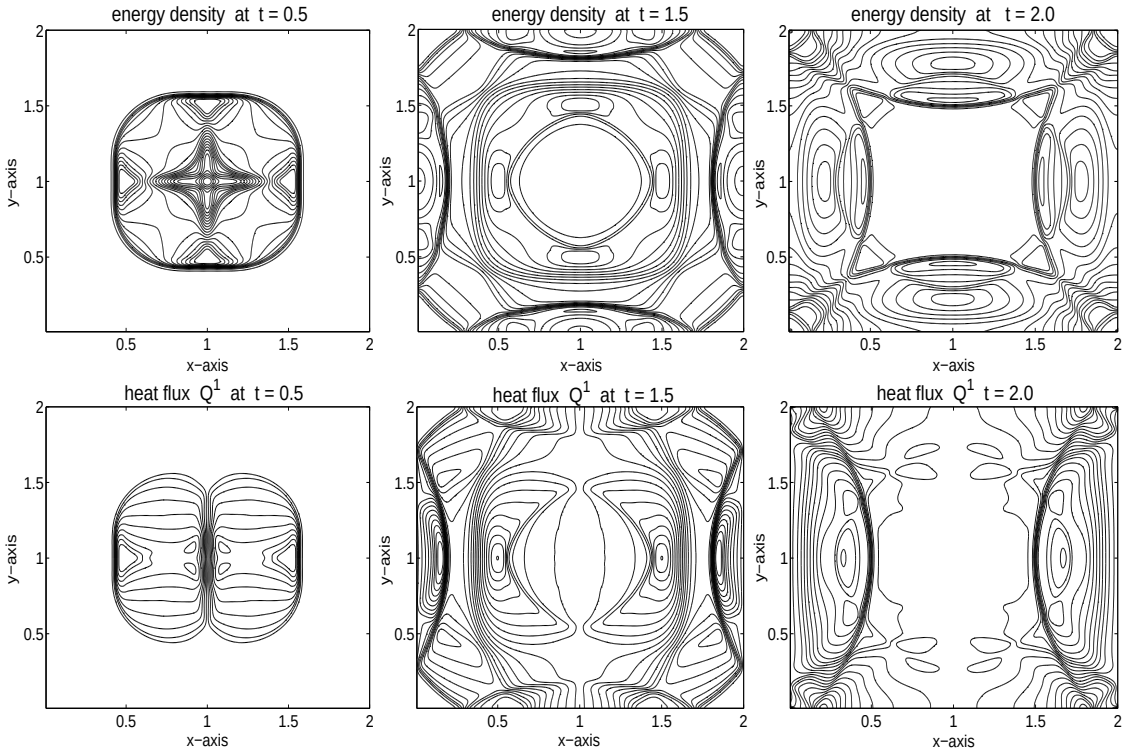

Figure 9: Example 5: Explosion in a box problem.

Jüttner [26] extended the non-relativistic kinetic theory of gases, which was developed by D. Bernoulli, Clausius, Maxwell and Boltzmann, to the domain of relativity. He succeeded in deriving the relativistic generalization of the Maxwellian equilibrium phase density. Later on this phase density and the whole relativistic kinetic theory was structured in a well organized Lorentz-invariant form, see Chernikov [4], [5], Müller [32] and the textbook of deGroot, van Leeuven and van Weert [6]. In the textbook of Weinberg [40] one can find a short introduction to special relativity and relativistic hydrodynamics with further literature also on the imperfect fluid (gas), see for example Eckart's seminal papers [19, 20, 21].

In [29, 27, 28, 31, 37] Kunik, Qamar and Warnecke have formulated two different kinetic schemes in order to solve the initial and boundary value problems for the *ultra-relativistic Euler equations* as well as in the general case.

The first kind of kinetic schemes are discrete in time but continuous in space. These schemes are explicit and unconditionally stable. Furthermore, the schemes are multi-dimensional and satisfy the weak form of conservation laws for mass, momentum, and energy, as well as an entropy inequality. The schemes preserve the positivity of particle density and pressure for all times and hence they are L^1-stable. Moreover, these schemes may be extended to account for boundary conditions, see [29, 27, 31, 37].

The second kind of kinetic schemes are discrete both in time and space, see [28, 37] and have an upwind conservative form. We use flux vector splitting in order to

calculate the free flight moment integrals. The structure of the light cone implies a natural CFL condition. These schemes are called kinetic flux vector splitting (KFVS) schemes which we have extended to the two-dimensional case by dimension splitting. We use a MUSCL-type data reconstruction to obtain second order accuracy.

In the following we restrict to the ultra-relativistic limit, where we meet a simpler mathematical structure. In particular, all moments are completely determined by surface integrals with respect to the unit sphere. Due to this fact, the ultra-relativistic Euler equations may be treated similar to the moment systems of the Boltzmann-Peierls equation.

3.2 The ultra-relativistic Euler equations

The coordinates with respect to a fixed reference frame are given by the 4-vector x^μ, $\mu \in \{0, 1, 2, 3\}$, where $x^0 = t$ is the observer time. The three vector $\mathbf{x} = x^i$, $i \in \{1, 2, 3\}$, denotes the spatial coordinates of any event x^μ. For simplicity we set $c = \hbar = k_B = 1$. Furthermore we assume that the metric tensor $g_{\mu\nu}$ is given by a diagonal matrix $g_{\mu\nu} = g^{\mu\nu} = \mathrm{diag}(1, -1, -1, -1)$.

The kinetic variable the 4-momentum of the gas particles $q^\mu = (q^0, \mathbf{q})$ with $\mathbf{q} = q^i$, $i \in \{1, 2, 3\}$. However, not all components of the 4-momentum are independent, because

$$q^\mu q_\mu = m^2, \tag{63}$$

where m is the rest mass of the particles. The invariant volume element $d\omega$ of the momentum space is given by

$$d\omega = \frac{1}{q_0} dq^1 dq^2 dq^3 = \frac{1}{q_0} d^3q. \tag{64}$$

The phase density $f(x^\mu, q^m) \equiv f(t, \mathbf{x}, \mathbf{q})$ gives the number density of particles in the element $d\omega$ at x^μ.

From now on we consider exclusively particles without rest mass, i.e. $m = 0$, so that

$$q_0 \equiv |\mathbf{q}| \quad \text{and} \quad d\omega = \frac{d^3q}{|\mathbf{q}|} \tag{65}$$

This is the ultra-relativistic limit, and the macroscopic quantities that appear in the relativistic Euler equations can be calculated from the following moments of the phase density

$$N^\mu = N^\mu(t, \mathbf{x}) = \int_3 q^\mu f(t, \mathbf{x}, \mathbf{q}) \frac{d^3q}{|\mathbf{q}|} \quad \text{and} \tag{66}$$

$$T^{\mu\nu} = T^{\mu\nu}(t, \mathbf{x}) = \int_3 q^\mu q^\nu f(t, \mathbf{x}, \mathbf{q}) \frac{d^3q}{|\mathbf{q}|}, \tag{67}$$

which give the particle 4-vector and the energy-momentum tensor, respectively. Furthermore we consider exclusively non-degenerate gas particles so that the entropy four vector is given by

$$S^\mu = S^\mu(t,\, \mathbf{x}) = -\int_3 q^\mu f(t,\, \mathbf{x},\, \mathbf{q}) \ln\left(f(t,\, \mathbf{x},\, \mathbf{q})\right) \frac{d^3q}{|\mathbf{q}|}. \tag{68}$$

There are conservation laws for N^μ, $T^{\mu\nu}$ and an inequality in conservative form for S^μ, viz.

$$\frac{\partial N^\mu}{\partial x^\mu} = 0\,, \quad \frac{\partial T^{\mu\nu}}{\partial x^\mu} = 0, \quad \frac{\partial S^\mu}{\partial x^\mu} \geq 0. \tag{69}$$

We read off from (66)-(69) the interpretations: N^0 - particle density, N^i - particle flux vector, T^{0j} - momentum density, T^{ij} - momentum flux, T^{00} - energy density, T^{i0} - energy flux, S^0 - entropy density, and S^i - entropy flux, where $i,\, j \in \{1,\, 2,\, 3\}$. We conclude from the symmetry $T^{\mu\nu} = T^{\nu\mu}$ that the momentum flux is equal to the energy flux. Note that the particle flux vector is not equal to the momentum density, as it is the case in the non-relativistic limit.

Next we introduce the macroscopic 4-velocity u^μ by

$$u^\mu = \frac{1}{n} N^\mu, \quad n = \sqrt{N^\nu N_\nu}, \tag{70}$$

so that $u^\mu u_\mu = 1$. We define the local rest frame of the gas by $u^\mu = (1, 0, 0, 0)$. We can use u^μ and the combination $h_{\mu\nu} = (u_\mu u_\nu - g_{\mu\nu})$ to define further macrospic fields that have a suggestive meaning in the local rest frame. These are $e = u_\mu u_\nu T^{\mu\nu}$ - internal energy density, $p = 1/3 h_{\mu\nu} T^{\mu\nu}$ - pressure, $Q_\mu = -h_{\mu\lambda} u_\nu T^{\lambda\nu}$ - heat flux, and $p_{<\mu\nu>} = (h_{\mu\lambda} h_{\nu\kappa} - 1/3 h_{\mu\nu} h_{\lambda\kappa}) T^{\lambda\kappa}$ - pressure deviator, where $p^{<\mu\nu>}$ denotes the trace free part of $p^{\mu\nu}$. There follows

$$N^\mu = n u^\mu \quad \text{and} \quad T^{\mu\nu} = e u^\mu u^\nu + p h^{\mu\nu} + Q^\mu u^\nu + Q^\nu u^\mu + p^{<\mu\nu>}. \tag{71}$$

In the ultra-relativistic limit we have $g_{\mu\nu} q^\mu q^\nu = 0$ and $(67)_2$ and $(71)_2$ imply $e = 3p$.

In the ultra-relativistic case, the phase density that maximizes the entropy density (68) in the local rest frame under the constraints of given values for n and e is called the ultra-relativistic Jüttner phase density, cf. [26, 27]. It reads

$$\begin{aligned} f_J\,(n,\, T,\, \mathbf{u},\, \mathbf{q}) &= \frac{n}{8\pi T^3} \exp\left(-\frac{u_\mu q^\mu}{T}\right) \\ &= \frac{n}{8\pi T^3} \exp\left(-\frac{|\mathbf{q}|}{T}\left(\sqrt{1+\mathbf{u}^2} - \mathbf{u}\cdot\frac{\mathbf{q}}{|\mathbf{q}|}\right)\right). \end{aligned} \tag{72}$$

Herein T denotes the temperature, which is defined by $T = p/n$.

Next we calculate the particle 4-vector and the energy-momentum tensor from the Jüttner phase density. We obtain $Q_\mu = 0$ and $p_{<\mu\nu>} = 0$ and the conservation laws

(69) formally transform into the ultra-relativistic Euler equations

$$\begin{aligned}
\frac{\partial}{\partial t}\left(n\sqrt{1+\mathbf{u}^2}\right)+\sum_{k=1}^{3}\frac{\partial}{\partial x^k}(n\,u^k) &= 0,\\
\frac{\partial}{\partial t}(4pu^i\sqrt{1+\mathbf{u}^2})+\sum_{k=1}^{3}\frac{\partial}{\partial x^k}\left(p\,\delta^{ik}+4pu^iu^k\right) &= 0,\\
\frac{\partial}{\partial t}\left(3p+4p\mathbf{u}^2\right)+\sum_{k=1}^{3}\frac{\partial}{\partial x^k}\left(4pu^k\sqrt{1+\mathbf{u}^2}\right) &= 0.
\end{aligned} \tag{73}$$

3.3 Kinetic Schemes

As mentioned in the introduction, the kinetic approach for the ultra-relativistic Euler equations consists of periods of free flight and update times. In particular, we prescribe a time step $\tau_M > 0$ and define the update times $t_m = m\,\tau_M$ for $m = 0, 1, 2, 3...$

The evolution during the periods of free flight is given by the collision transport equation which reads in the ultra-relativistic case

$$\frac{\partial f}{\partial t}+\sum_{k=1}^{3}\frac{q^k}{|\mathbf{q}|}\frac{\partial f}{\partial x^k}=0. \tag{74}$$

Since we cannot expect the phase densities to be continuous at the update times, we have to distinguish between the left-hand and right-hand limits w.r.t. time. We thus define

$$f_m^{\pm}(\mathbf{x},\,\mathbf{q}) := \lim_{\tau\searrow 0+} f(t_m\pm\tau,\,\mathbf{x},\,\mathbf{q}). \tag{75}$$

Within the m-th period of free flight, i.e $t_{m-1} < t \le t_m$, the moments of f are given by

$$N^\mu(t_{m-1}+\tau,\,\mathbf{x}) = \int_3 q^\mu\, f_{m-1}^+(\mathbf{x}-\tau\frac{\mathbf{q}}{|\mathbf{q}|},\,\mathbf{q})\,\frac{d^3q}{|\mathbf{q}|}, \tag{76}$$

$$T^{\mu\nu}(t_{m-1}+\tau,\,\mathbf{x}) = \int_3 q^\mu q^\nu\, f_{m-1}^+(\mathbf{x}-\tau\frac{\mathbf{q}}{|\mathbf{q}|},\,\mathbf{q})\,\frac{d^3q}{|\mathbf{q}|}, \tag{77}$$

whereas the fields n, $\mathbf{u}$, T, and p are determined by the algebraic equations

$$n=\sqrt{N^\mu N_\mu},\quad u^\mu=\frac{1}{n}N^\mu,\quad T=\frac{1}{3n}u_\mu u_\nu\,T^{\mu\nu},\quad p=nT. \tag{78}$$

At the update time t_m we use the free flight density f_m^- in order to calculate f_m^+ as a Jüttner phase density

$$f_m^+(\mathbf{x},\,\mathbf{q}) = f_J\Big(\tilde{n}_m(\mathbf{x}),\,\tilde{T}_m(\mathbf{x}),\,\tilde{\mathbf{u}}_m(\mathbf{x}),\,\mathbf{q}\Big). \tag{79}$$

We choose the fields $\tilde{n}_m$, $\tilde{T}_m$, and $\tilde{\mathbf{u}}_m$ so that the densities N^0 and $T^{0\nu}$ are conserved across the update times. In particular, for all t_m and all $\mathbf{x}$ we have to ensure the continuity conditions

$$\int_3 q^0 \, f_m^+(\mathbf{x},\, \mathbf{q}) \, \frac{d^3q}{|\mathbf{q}|} \;=\; \int_3 q^0 \, f_m^-(\mathbf{x},\, \mathbf{q}) \, \frac{d^3q}{|\mathbf{q}|}, \tag{80}$$

$$\int_3 q^0 q^\nu \, f_m^+(\mathbf{x},\, \mathbf{q}) \, \frac{d^3q}{|\mathbf{q}|} \;=\; \int_3 q^0 q^\nu \, f_m^-(\mathbf{x},\, \mathbf{q}) \, \frac{d^3q}{|\mathbf{q}|} \tag{81}$$

It is important to note that the conditions (80) and (81) guaranty the continuity of the densities N^0 and $T^{0\nu}$ at the update times, but they do not imply the continuity of the fields n, T, p, and $\mathbf{u}$ at the update times. We mention that the fields $\tilde{n}_m$, $\tilde{T}_m$ $\tilde{p}_m$, and $\tilde{\mathbf{u}}_m$ turn out be the right-hand limits of n, T, p, and $\mathbf{u}$, respectively.

The update procedure maximizes the entropy in any point $(t_m,\, \mathbf{x})$ under the constraints of prescribed densities. For this reason we call the update times *maximization times*.

From (79), (80), and (81) we may derive the following explicit expressions for $\tilde{\mathbf{u}}_m$, $\tilde{n}_m$, and $\tilde{T}_m$

$$\tilde{u}_m^k = \frac{T_m^{0k}}{\sqrt{4\tilde{p}_m\,(\tilde{p}_m + T_m^{00})}}, \quad \tilde{n}_m = \frac{N_m^0}{\sqrt{1+\tilde{\mathbf{u}}_m^2}}, \quad \tilde{T}_m = \frac{\tilde{p}_m}{\tilde{n}_m}. \tag{82}$$

Here $N_m^0(\mathbf{x}) = N^0(t_m,\, \mathbf{x})$ and $T_m^{0\nu}(\mathbf{x}) = T^{0\nu}(t_m,\, \mathbf{x})$ are the densities at the update time t_m and $\tilde{p}_m$ is given by

$$\tilde{p}_m \;=\; \frac{1}{3}\left(-T_m^{00} + \sqrt{4(T_m^{00})^2 - 3\sum_{k=1}^{3}(T_m^{0k})^2}\right). \tag{83}$$

3.3.1 Reduction to surface integrals

The moment integrals (76) and (77) may be simplified as follows. We split the microscopic variable $\mathbf{q}$ into its length $|\mathbf{q}|$ and into its direction

$$\mathbf{w} = (w^1, w^2, w^3)^T = \frac{\mathbf{q}}{|\mathbf{q}|} \in S^2, \tag{84}$$

where S^2 denotes the unit sphere. Due to the ultra-relativistic structure of the moment integrals in (76) and (77), we may carry out the integration with respect to $|\mathbf{q}|$. There result the following expressions

$$N^\mu(t_m + \tau,\, \mathbf{x}) \;=\; \oint_{S^2} w^\mu \, \Phi_m(\mathbf{x} - \tau\mathbf{w},\, \mathbf{w}) \, dS(\mathbf{w}), \tag{85}$$

$$T^{\mu\nu}(t_m + \tau, \mathbf{x}) \;=\; \oint_{S^2} w^\mu w^\nu \Psi_m(\mathbf{x} - \tau\mathbf{w},\, \mathbf{w}) \, dS(\mathbf{w}), \tag{86}$$

where $w^0 = 1$ and $\mu, \nu \in \{0,\, 1,\, 2,\, 3\}$ and

$$\Phi_m(\mathbf{x},\, \mathbf{w}) = \frac{1}{4\pi} \frac{\tilde{n}_m(\mathbf{x})}{\left(\sqrt{1 + \tilde{\mathbf{u}}_m^2(\mathbf{x})} - \mathbf{w} \cdot \tilde{\mathbf{u}}_m(\mathbf{x})\right)^3} \tag{87}$$

$$\Psi_m(\mathbf{x},\, \mathbf{w}) = \frac{3}{4\pi} \frac{\tilde{p}_m(\mathbf{x})}{\left(\sqrt{1 + \tilde{\mathbf{u}}_m^2(\mathbf{x})} - \mathbf{w} \cdot \tilde{\mathbf{u}}_m(\mathbf{x})\right)^4}. \tag{88}$$

The functions Φ_m and Ψ_m are the counterparts to the reduced phase densities for the Boltzmann-Peierls equation, cf. Section 2.2.

The surface integrals in (85) and (86) reflect the fact that in the ultra-relativistic case the particles are moving on the surface of the light cone.

3.3.2 Kinetic scheme in one space dimension

Here we consider phase densities f that do not depend on x^2 and x^3, and we will show that this restriction gives rise to a further simplification of the kinetic scheme.

In the following we write $x = x^1$,

$$n = n(t,\, x), \quad \mathbf{u} = (u(t,\, x),\, 0,\, 0), \quad p = p(t,\, x), \quad T = T(t,\, x), \tag{89}$$

and so on. Next we introduce new variables $-1 \leq \xi \leq 1$ and $0 \leqq \varphi \leqq 2\pi$ by

$$w^1 = \xi\,, \qquad w^2 = \sqrt{1 - \xi^2}\sin\varphi\,, \qquad w^3 = \sqrt{1 - \xi^2}\cos\varphi. \tag{90}$$

The surface element then becomes $dS(\mathbf{w}) = d\xi d\varphi$. Now we can carry out the integration with respect to the angular φ in (85) and (86) and we obtain

$$N^\mu(t_m + \tau,\, x) = \int_{-1}^{1} w^\mu \Phi_m(x - \tau\xi,\, \xi)\, d\xi, \tag{91}$$

$$T^{\mu\nu}(t_m + \tau,\, x) = \int_{-1}^{1} w^\mu w^\nu \Psi_m(x - \tau\xi,\, \xi)\, d\xi, \tag{92}$$

where

$$\Phi_m(x,\, \xi) = \frac{1}{2} \frac{\tilde{n}_m(x)}{\left(\sqrt{1 + \tilde{u}_m^2(x)} - \xi\tilde{u}_m(x)\right)^3}, \tag{93}$$

$$\Psi_m(x,\, \xi) = \frac{3}{2} \frac{\tilde{p}_m(x)}{\left(\sqrt{1 + \tilde{u}_m^2(x)} - \xi\tilde{u}_m(x)\right)^4}. \tag{94}$$

3.4 Numerical Examples

3.4.1 Problem 1: Relativistic shock tube

The initial data are

$$(n, u, p) = \begin{cases} (5.0, 0.0, 10.0) & \text{if } x < 0.5\,, \\ (1.0, 0.0, 0.5) & \text{if } x \geq 0.5\,. \end{cases}$$

The spatial domain is taken as $[0, 1]$ with 400 mesh elements and the final time is $t = 0.5$. For the kinetic scheme we consider 100 maximization times. This problem involves the formation of an intermediate state bounded by a shock wave propagating to the right and a transonic rarefaction wave propagating to the left. The fluid in the intermediate state moves at a mildly relativistic speed ($v = 0.58c$) to the right. Flow particles accumulate in a dense shell behind the shock wave compressing the fluid and heating it. Figures 10 show the particle density n, fluid velocity $v = \frac{u}{\sqrt{1+u^2}}$ and pressure p.

3.4.2 Problem 2: Implosion in a box

In this example we consider a two-dimensional Riemann problem inside a square box of sides length 2, with reflecting walls. Initially the velocities are zero. The pressure is 10 and density is 4 inside a small square box of sides length 0.5 in the center of the large box, while pressure and density are unity elsewhere. The results are shown at $t = 3.0$ in Figure 11. We have used 400×400 mesh points.

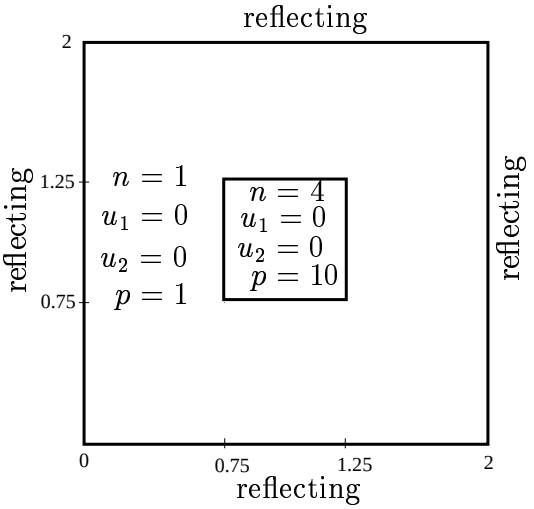

References

[1] P.L. Bhatnagar, E.P. Gross, and M. Krook, *A model for collision processes in gases. i. small amplitude processes in charged and neutral one-component systems*, Phys. Rev. **94** (1954), 511–525.

[2] J. Callaway, *Quantum theory of the solid state*, Academic Press, San Diego, 1991.

[3] C. Cercignani, *The Boltzmann equation and its applications*, Applied Mathematical Sciences, vol. 67, Springer, New York, 1988.

[4] N.A. Chernikov, *Equilibrium distribution of the relativistic gas*, Acta Phys. Pol. **26** (1964), 1069–1092.

[5] ———, *Microscopic foundation of relativistic hydrodynamics*, Acta Phys. Pol. **27** (1964), 465–489.

[6] S.R. deGroot, W.A. van Leeuven, and Ch.G. van Weert, *Relativistic kinetic theory: Principles and applications*, North Holland, Amsterdam, 1980.

[7] S.M. Deshpande, *A second order accurate, kinetic-theory based, method for inviscid compressible flows*, NASA Langley Tech. Paper (1986), no. 2613.

[8] ———, *Kinetic flux splitting schemes*, Computational Fluid Dynamics Review (M. Hafez and K. Oshima, eds.), John Wiley & sons, 1995.

[9] W. Dreyer, M. Herrmann, and M. Kunik, *Kinetic solutions of the Boltzmann-Peierls equation and its moment systems*, Preprint, no. 709, Weierstrass Institute Berlin (WIAS), 2001, to appear in Cont. Mech. Thermdyn.

[10] ———, *Kinetic schemes and initial boundary value problems*, Transport Theory in Statistical Physics **31** (2002), 1–33.

[11] W. Dreyer, M. Junk, and M. Kunik, *On the approximation of kinetic equations by moment systems*, Nonlinearity **14** (2001), 881–906.

[12] W. Dreyer and M. Kunik, *The maximum entropy principle revisited*, Cont. Mech. Thermodyn. **10** (1998), 331–347.

[13] ———, *Reflections of Eulerian shock waves at moving adiabatic boundaries*, Monte Carlo Methods and Applications **4.3** (1998), 231–252.

[14] ———, *Initial and boundary value problems of hyperbolic heat conduction*, Cont. Mech. Thermodyn. **11.4** (1999), 227–245.

[15] ———, *Hyperbolic heat conduction*, Trends in applications of Mathematics to Mechanics, CRC Monographs and Surveys in Pure and Applied Mathematics, vol. 109, Chapman & Hall, 2000.

[16] W. Dreyer and S. Qamar, *Kinetic flux-vector splitting schemes for the hyperbolic heat conduction*, Preprint, no. 861, Weierstrass Institute Berlin (WIAS), 2003.

[17] ———, *Second order accurate explicit finite volume schemes for the solution of Boltzmann-Peierls equation*, Preprint, no. 860, Weierstrass Institute Berlin (WIAS), 2003.

[18] W. Dreyer and H. Struchtrup, *Heat pulse experiments revisited*, Cont. Mech. Thermodyn. **5** (1993), 1–50.

[19] C. Eckart, *The thermodynamics of irreversible process I: The simple fluid*, Phys. Rev. **58** (1940), 267–269.

[20] ———, *The thermodynamics of irreversible process II: Fluid mixtures*, Phys. Rev. **58** (1940), 269–275.

[21] ———, *The thermodynamics of irreversible process III: Relativistic theory of the simple fluid*, Phys. Rev. **58** (1940), 919–928.

[22] E. Godlewski and P.A. Raviart, *Numerical approximation of hyperbolic systems of conservation laws*, Applied Mathematical Sciences, vol. 118, Springer, New York, 1996.

[23] G.-S. Jaing and E. Tadmor, *Non-oscillatory central schemes for multidimensional hyperbolic conservation laws*, SIAM J. Sci. Comput. **19** (1998), 1892–1917.

[24] M. Junk, *Kinetic schemes: A new approach and applications*, Shaker-Verlag, 1997.

[25] ———, *Domain of definition of Levermore's five-moment system*, J. Stat. Phys. **93** (1998), 1143–1167.

[26] F. Jüttner, *Das Maxwellsche Gesetz der Geschwindigkeitsverteilung in der Relativtheorie*, Ann. Phys. **34** (1911), 856–882.

[27] M. Kunik, S. Qamar, and G. Warnecke, *Kinetic schemes for the relativistic gas dynamics*, Preprint, no. 21, Otto-von-Guericke University Magdeburg, 2002.

[28] ———, *A BGK-type kinetic flux- vector splitting schemes for the ultra-relativistic Euler equations*, Preprint, no. 4, Otto-von-Guericke University Magdeburg, 2003.

[29] ———, *Kinetic schemes for the ultra-relativistic Euler equations*, J. Comput. Phys. **187** (2003), 572–596.

[30] ———, *A reduction of the Boltzmann-Peierls equation*, Preprint, no. 6, Otto-von-Guericke University Magdeburg, 2003.

[31] ———, *Second order accurate kinetic schemes for the ultra-relativistic Euler equations*, Preprint, no. 18, Otto-von-Guericke University Magdeburg, 2003.

[32] I. Müller, *Speeds of propagation in classical and relativistic extended thermodynamics*, Max Planck Institute for Gravitational Physics, 1999.

[33] I. Müller and T. Ruggeri, *Rational extended thermodynamics*, Springer, New York, 1998.

[34] H. Nessyahu and E. Tadmor, *Non-oscillatory central differencing fo hyperbolic conservation laws*, SIAM J. Comput. Phys. **87** (1990), 408–448.

[35] R.E. Peierls, *Quantum theory of solids*, Oxford University Press, London, 1995.

[36] B. Perthame, *Boltzmann type schemes for gas dynamics and the entropy property*, SIAM J. Numer. Anal. **27.6** (1990), 1405–1421.

[37] S. Qamar, *Kinetic schemes for the relativistic hydrodynamics*, Ph.D. thesis, Faculty of Mathematics, Otto-von-Guericke University Magdeburg, 2003.

[38] R.D. Reitz, *One-dimensional compressible gas dynamics calculations using the Boltzmann equation*, J. Comput. Phys. **42** (1981), 108–123.

[39] E.F. Toro, *Riemann solvers and numerical method for fluid dynamics*, Springer, New York, 1999.

[40] S. Weinberg, *Gravitation and cosmology*, Wiley, New York, 1972.

[41] K. Xu, *Gas kinetic schemes for unsteady compressible flow simulations*, VKI Fluid Dynamics Lecture Series **1998-03** (1998).

[42] ———, *Gas evolution dynamics in Godunov-type schemes and analysis of numerical shock instability*, ICASE Report (1999), no. 99-6.

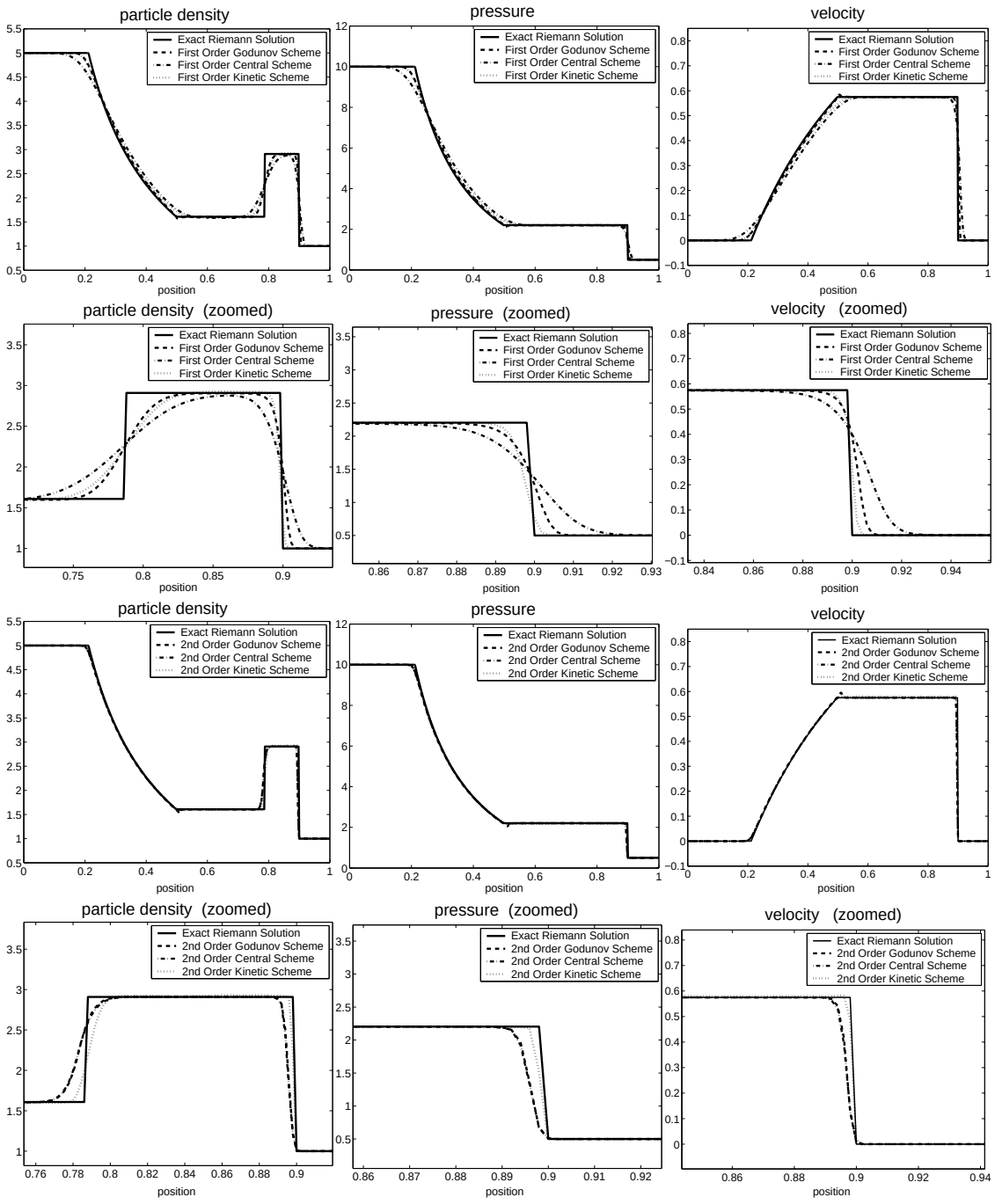

Figure 10: Problem 1: Comparison of the results at time $t = 0.5$.

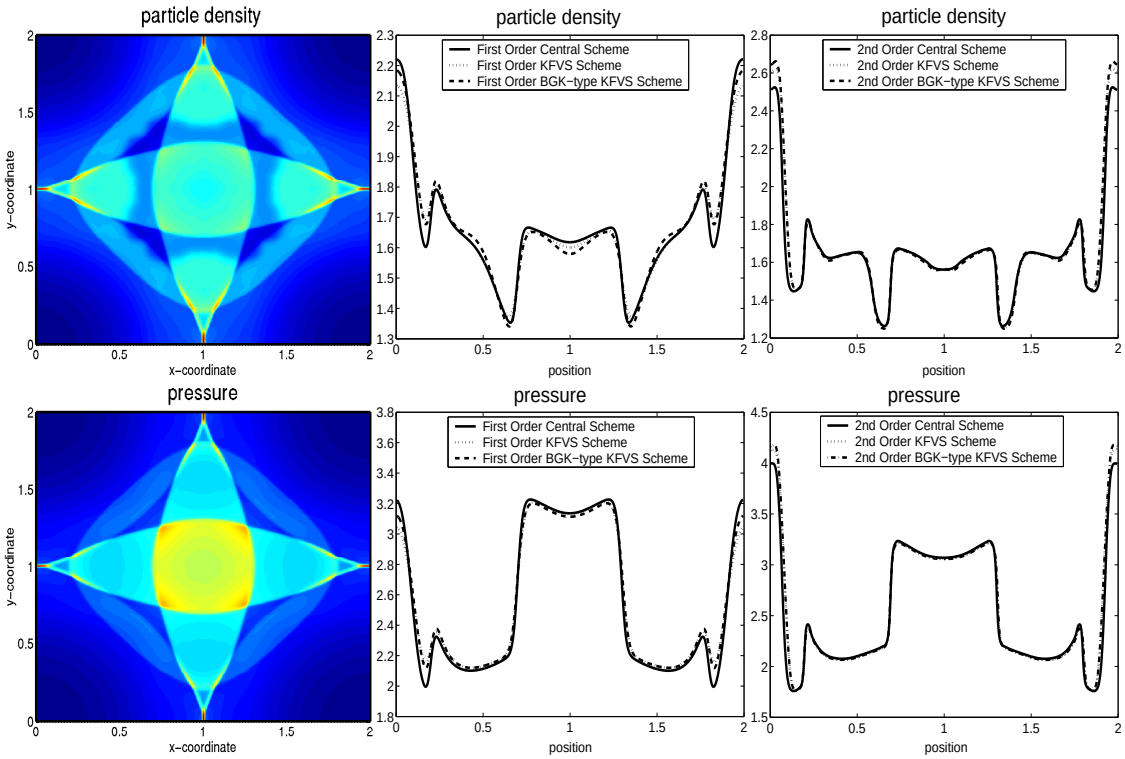

Figure 11: Problem 2: Implosion in a box at $t = 3.0$.